

Adaptive Smoothing with Ambiguity Fixation for GNSS Post-Processing

Greiff, Marcus; Berntorp, Karl; Di Cairano, Stefano

TR2023-083 July 08, 2023

Abstract

We propose a complete post-processing solution for GNSS (global navigation satellite system) positioning leveraging linear-regression Kalman filtering methods, employed in a Rauch-Tung-Striebel (RTS) smoothing context, and adapting the model parameters in an expectation maximization (EM) framework. In particular, we (i) discuss the effects of using different moment approximations in the smoother; (ii) demonstrate that it is advantageous to fixate the integer ambiguities on the smoothing posterior; and (iii) show that the proposed method is viable for a wide range of GNSS measurement models, including single difference, double difference, and ionosphere-free combinations of the multi-band GNSS observations.

World Congress of the International Federation of Automatic Control (IFAC) 2023

Adaptive Smoothing with Ambiguity Fixation for GNSS Post-Processing

Marcus Greiff* Stefano Di Cairano* Karl Berntorp*

* Mitsubishi Electric Research Labs, 02139 Cambridge, MA, USA
(e-mail: greiff@merl.com, {karl.o.berntorp,dicairano}@ieee.org).

Abstract: We propose a complete post-processing solution for GNSS (global navigation satellite system) positioning leveraging linear-regression Kalman filtering methods, employed in a Rauch-Tung-Striebel (RTS) smoothing context, and adapting the model parameters in an expectation maximization (EM) framework. In particular, we (i) discuss the effects of using different moment approximations in the smoother; (ii) demonstrate that it is advantageous to fixate the integer ambiguities on the smoothing posterior; and (iii) show that the proposed method is viable for a wide range of GNSS measurement models, including single difference, double difference, and ionosphere-free combinations of the multi-band GNSS observations.

Keywords: Kalman filtering, RTS Smoothing, GNSS positioning, Parameter Estimation

1. INTRODUCTION

The *GNSS positioning problem* concerns the estimation of a receiver’s states from a set of pseudo-range, phase-range, and potentially also Doppler measurements, acquired from one or several constellations of satellites (see Teunissen (1997)). The measurement equation, from which the receiver state is inferred, is time-varying, nonlinear in the position of the receiver, and incorporates various biases, as discussed in Leick et al. (2015). Some of these are integer-valued, commonly referred to as *ambiguities* (see, e.g., Teunissen et al. (1995)). If leveraging this information and *fixing* the integers, the estimation accuracy generally improves at the cost of a significantly more complex estimation problem (see Teunissen (1997)). The problem is often considered in a filtering setting, as in Berntorp et al. (2018); Greiff et al. (2021); Odolinski and Teunissen (2016); Takasu and Yasuda (2010); Zhao et al. (2014). However, the GNSS data are often stored in batches in the RINEX format, and there is significant interest in post-processing such data, amounting to a smoothing problem.

With this motivation, we consider smoothing for models

$$\mathbf{x}_{k+1} = \mathbf{A}_k \mathbf{x}_k + \mathbf{B}_k^{\mathbb{R}} \mathbf{q}_k + \mathbf{B}_k^{\mathbb{Z}} \mathbf{s}_k, \quad (1a)$$

$$\mathbf{y}_k = \mathbf{g}_k(\mathbf{x}_k) + \mathbf{C}_k \mathbf{x}_k + \mathbf{r}_k, \quad (1b)$$

where the noise terms are independent and additive,

$$p(\mathbf{q}_k, \mathbf{r}_k, \mathbf{s}_k) = \mathcal{N}(\mathbf{q}_k; \mathbf{0}, \mathbf{Q}_k^{\mathbb{R}}(\boldsymbol{\theta})) \mathcal{N}(\mathbf{r}_k; \mathbf{0}, \mathbf{R}_k) \mathcal{J}(\mathbf{s}_k; a\mathbf{1}, b\mathbf{1}),$$

where $\boldsymbol{\theta}$ is a parameter vector; \mathcal{N} denotes the Gaussian density; and \mathcal{J} is the integer jump process in Greiff et al. (2021). Here, elements of $[\mathbf{s}_k]_i \in [-a, a] \subset \mathbb{Z}$ are realized as nonzero integers with a probability b . The notion is clarified in Sec. 2 and the problem is defined as follows.

Problem 1. Given a $p(\mathbf{x}_{k+1}|\mathbf{x}_k)$ and a measurement model $p(\mathbf{y}_k|\mathbf{x}_k)$, with $\mathbf{x}_k = (\mathbf{x}_k^{\mathbb{R}}, \mathbf{x}_k^{\mathbb{Z}}) \in \mathbb{R}^m \times \mathbb{Z}^n$, compute a fixed-interval approximate Gaussian smoothing posterior $p(\mathbf{x}_k^{\mathbb{R}}|\mathbf{x}_{0:K}^{\mathbb{Z}}, \mathbf{y}_{0:K}) \approx \mathcal{N}(\mathbf{x}_k^{\mathbb{R}}; \check{\mathbf{m}}_{k|K}, \check{\boldsymbol{\Sigma}}_{k|K})$ conditioned an associated fixed integer trajectory $\mathbf{x}_{0:K}^{\mathbb{Z}}$ and a set of all measurements $\mathbf{y}_{0:K}$ (where $0 \leq k \leq K$), and estimate $\boldsymbol{\theta}$.

Smoothing for GNSS post-processing has been analyzed rigorously in the literature, with methods generally involving smoothing passes with *known* model parameters $\boldsymbol{\theta}$. Typically, this is done using the Rauch-Tung-Striebel (RTS) framework (see Rauch et al. (1965)), or Fraser-Potter (FP) smoothing (see Fraser and Potter (1969)), with explicit linearizations (the smoothing equivalent of an extended Kalman filter) under known model parameters. For instance, the work in Vaclavovic and Dousa (2015) considers RTS smoothing in a precise-point positioning (PPP) setting, without adapting the model parameters.

In this paper, we propose an iterative algorithm for to approximately solve Problem 1, inspired by the dual-density filtering in Greiff et al. (2021). The algorithm consists of two main steps. The first is a generalized RTS smoother, used to compute the posterior $p(\mathbf{x}_k|\mathbf{y}_{0:K})$ given some $\boldsymbol{\theta}^{(i)}$, using the partially linear moment approximations in Greiff et al. (2020). The second step consists of an update law of the parameters using a structured expectation maximization (EM) in which the objective function is defined in the smoothing posterior (see Särkkä (2013)), facilitating a safe and efficient adaptive post-processing algorithm.

Contributions We demonstrate that parameter adaptation, when done in the EM framework, can yield significant improvements in GNSS post-processing. We also show that fast and efficient smoothing algorithms can be implemented using various extended- and/or linear-regression Kalman filtering (LRKF) moment approximations if the linear substructures in the model are exploited. We discuss the effects on integer fixation accuracy when done with respect to the filtering and smoothing posteriors, respectively. Finally, we give examples considering models with multiple frequency bands, double- or single-difference measurements, and ionosphere-free observations.

2. PRELIMINARIES

Vectors are denoted by $\mathbf{x} \in \mathbb{R}^n$ with $[\mathbf{x}]_i$ denoting the i^{th} element of \mathbf{x} . Matrices are indicated in bold font, \mathbf{X} , and

the element on row i and column j of \mathbf{X} is written $[\mathbf{X}]_{ij}$. The notation $\mathbf{v} \sim \mathcal{N}(\mathbf{v}; \mathbf{m}^v, \Sigma^{vv})$ indicates that \mathbf{v} is Gaussian distributed random variable with mean \mathbf{m}^v and covariance Σ^{vv} , and the super-indices are often dropped for brevity. The bar (\cdot) is used to indicate a random variable if necessary, but often dropped to clarify the presentation. Given the set of measurements $\mathbf{y}_{0:k} = \{\mathbf{y}_0, \dots, \mathbf{y}_k\}$, we let $p(\mathbf{x}_k | \mathbf{y}_{0:k}) \approx \mathcal{N}(\mathbf{x}_k; \mathbf{m}_{k|k}, \Sigma_{k|k})$ denote a marginal filtering posterior; $p(\mathbf{x}_k | \mathbf{y}_{0:K}) \approx \mathcal{N}(\mathbf{x}_k; \mathbf{m}_{k|K}, \Sigma_{k|K})$ denote a marginal smoothing posterior; and take $\mathcal{N}(\mathbf{x}_k^{\text{R}} | \check{\mathbf{m}}_k, \check{\Sigma}_k)$ to denote a *fixed* estimate. To make the exposition clear, we let $(\cdot)_{k|k} = (\cdot)_k$ in the filter posterior, and distinguish the moments of the smoothing posterior with $(\cdot)_{k|K} = (\cdot)_k^s$.

2.1 Linear RTS Smoothing

If relaxing the integer constraint such that $\mathbf{x}_k \in \mathbb{R}^{m+n}$, and assuming knowledge of the parameters $\boldsymbol{\theta}$ (hence omitted), the solution to Problem 1 is given by the Bayesian optimal smoothing equations (see, e.g., Kitagawa (1987)),

$$p(\mathbf{x}_{k+1} | \mathbf{y}_{0:k}) = \int p(\mathbf{x}_{k+1} | \mathbf{x}_k) p(\mathbf{x}_k | \mathbf{y}_{0:k}) d\mathbf{x}_k \quad (2a)$$

$$p(\mathbf{x}_k | \mathbf{y}_{0:K}) = p(\mathbf{x}_k | \mathbf{y}_{0:k}) \int \frac{p(\mathbf{x}_{k+1} | \mathbf{x}_k) p(\mathbf{x}_{k+1} | \mathbf{y}_{0:K})}{p(\mathbf{x}_{k+1} | \mathbf{y}_{0:k})} d\mathbf{x}_{k+1} \quad (2b)$$

For a Gaussian prior $\mathcal{N}(\mathbf{x}_0; \mathbf{m}_0, \Sigma_0)$, and a linear time-varying (LTV) motion model

$$\mathbf{x}_{k+1} = \mathbf{A}_k \mathbf{x}_k + \mathbf{q}_k, \quad \mathbf{q}_k \sim \mathcal{N}(\mathbf{0}, \mathbf{Q}_k), \quad (3a)$$

$$\mathbf{y}_k = \mathbf{C}_k \mathbf{x}_k + \mathbf{r}_k, \quad \mathbf{r}_k \sim \mathcal{N}(\mathbf{0}, \mathbf{R}_k), \quad (3b)$$

the Chapman-Kolmogorov equation in (2a) and subsequent conditioning on the new measurements results in the Kalman filter (KF). In the notation of Särkkä (2013), we let $p(\mathbf{x}_k | \mathbf{y}_{0:k}) = \mathcal{N}(\mathbf{x}_k; \mathbf{m}_k, \Sigma_k)$ be the filtering posterior. From (2b), the smoothing posterior can be obtained by backward pass (BP) from $\mathbf{m}_{K}^s = \mathbf{m}_K, \Sigma_K^s = \Sigma_K$, as

$$\mathbf{G}_k^s = \Sigma_k \mathbf{A}_k^\top (\Sigma_{k|k-1})^{-1} \quad (4a)$$

$$\mathbf{m}_k^s = \mathbf{m}_k + \mathbf{G}_k^s (\mathbf{m}_{k+1}^s - \mathbf{m}_{k|k-1}) \quad (4b)$$

$$\Sigma_k^s = \Sigma_k + \mathbf{G}_k^s (\Sigma_{k+1}^s - \Sigma_{k|k-1}) (\mathbf{G}_k^s)^\top, \quad (4c)$$

with a smoothing posterior $p(\mathbf{x}_k | \mathbf{y}_{0:K}) = \mathcal{N}(\mathbf{x}_k; \mathbf{m}_k^s, \Sigma_k^s)$. This is the common Rauch-Tung-Striebel (RTS) smoother.

2.2 Partially Linear RTS smoothing

If the estimation model is nonlinear with additive noise,

$$\mathbf{x}_{k+1} = \mathbf{f}_k(\mathbf{x}_k) + \mathbf{q}_k, \quad \mathbf{q}_k \sim \mathcal{N}(\mathbf{0}, \mathbf{Q}_k), \quad (5a)$$

$$\mathbf{y}_k = \mathbf{h}_k(\mathbf{x}_k) + \mathbf{r}_k, \quad \mathbf{r}_k \sim \mathcal{N}(\mathbf{0}, \mathbf{R}_k), \quad (5b)$$

the RTS smoother can be employed with first-order linearizations, under the assumption that the filtering and smoothing posteriors are both approximately Gaussian.

However, we will be dealing with a linear prediction model in (3a), and a partially linear measurement model, where

$$\mathbf{h}(\mathbf{x}_k) = \mathbf{g}_k(\mathbf{z}_k) + \mathbf{C}_k \mathbf{x}_k, \quad (6)$$

and \mathbf{z}_k is a subset of the states in \mathbf{x}_k . As such, we employ the partially linear moment approximations in Greiff et al. (2020) and modify the RTS smoother by assuming

$$p(\mathbf{x}_k; \mathbf{y}_k | \mathbf{y}_{0:k-1}) \approx \mathcal{N} \left(\begin{bmatrix} \mathbf{x}_k \\ \mathbf{y}_k \end{bmatrix}; \begin{bmatrix} \mathbf{m}_{k|k-1} \\ \mathbf{m}_{k|k-1}^y \end{bmatrix}, \begin{bmatrix} \Sigma_{k|k-1} & \Sigma_{k|k-1}^{\mathbf{x}\mathbf{y}} \\ \star & \Sigma_{k|k-1}^{\mathbf{y}\mathbf{y}} \end{bmatrix} \right)$$

directly approximating the moment integrals

$$\mathbf{m}_{k|k-1}^y = \int \mathbf{h}(\mathbf{x}_k) \mathcal{N}(\mathbf{x}_k; \mathbf{m}_{k|k-1}, \Sigma_{k|k-1}) d\mathbf{x}_k, \quad (7a)$$

$$\Sigma_{k|k-1}^{\mathbf{x}\mathbf{y}} = \int [\mathbf{x}_k - \mathbf{m}_{k|k-1}] [\mathbf{h}(\mathbf{x}_k) - \mathbf{m}_{k|k-1}^y]^\top \times \mathcal{N}(\mathbf{x}_k; \mathbf{m}_{k|k-1}, \Sigma_{k|k-1}) d\mathbf{x}_k, \quad (7b)$$

$$\Sigma_{k|k-1}^{\mathbf{y}\mathbf{y}} = \int [\mathbf{h}(\mathbf{x}_k) - \mathbf{m}_{k|k-1}^y] [\mathbf{h}(\mathbf{x}_k) - \mathbf{m}_{k|k-1}^y]^\top \times \mathcal{N}(\mathbf{x}_k; \mathbf{m}_{k|k-1}, \Sigma_{k|k-1}) d\mathbf{x}_k + \mathbf{R}_k, \quad (7c)$$

and subsequently performing the KF update with

$$\mathbf{K}_k = \Sigma_{k|k-1}^{\mathbf{x}\mathbf{y}} (\Sigma_{k|k-1}^{\mathbf{y}\mathbf{y}})^{-1}, \quad (8a)$$

$$\mathbf{m}_k = \mathbf{m}_{k|k-1} + \mathbf{K}_k (\mathbf{y}_k - \mathbf{m}_{k|k-1}^y), \quad (8b)$$

$$\Sigma_k = \Sigma_{k|k-1} - \mathbf{K}_k (\Sigma_{k|k-1}^{\mathbf{x}\mathbf{y}})^\top, \quad (8c)$$

Remark 1. Note that the measurement model does not appear in the RTS backward pass in (4). If the model retains linearity in the prediction model, the backward pass does not require burdensome approximations even if the measurement model is (partially) nonlinear.

In light of Remark 1, we only need to evaluate (7) in the forward pass of the RTS smoother under the assumption of a linear motion model. Furthermore, if the measurements are partially linear as in (6), we can leverage (Greiff et al., 2020, Proposition 1) to implement an RTS smoother to approximate the integrals in (7) with the number of integration points scaling with $\dim(\mathbf{z}_k)$ instead of $\dim(\mathbf{x}_k)$. We refer to this family of smoothers as Partially Linear RTS smoothers (PL-RTS), prefacing this with UT when using the unscented transform given in Wan and Van Der Merwe (2000); and SR when using the Spherical Radial rules of the Cubature Kalman filter in Arasaratnam (2009).

2.3 Structured Expectation Maximization

We briefly describe the expectation-maximization (EM) and refer to (Särkkä, 2013, Section 12.2.3) for additional details. The idea of EM is to define an arbitrary probability distribution over the states $q(\mathbf{x}_{0:K})$, and lower-bound the negative log-likelihood of the measurements $\mathbf{y}_{0:K}$ given $\boldsymbol{\theta}$,

$$\begin{aligned} \mathcal{L}(\boldsymbol{\theta}) &= -\log p(\mathbf{y}_{0:K} | \boldsymbol{\theta}) \\ &\leq -\int q(\mathbf{x}_{0:K}) \log \frac{p(\mathbf{y}_{0:K}, \mathbf{x}_{0:K} | \boldsymbol{\theta})}{q(\mathbf{x}_{0:K})} d\mathbf{x}_{0:K}, \end{aligned} \quad (9)$$

and minimize the left-hand side (LHS) by minimizing the upper bound on the right-hand side (RHS). The appeal of this idea lies in that the LHS in (9) may be a complicated function in $\boldsymbol{\theta}$, while the RHS (9) under certain conditions and choices of q can be expressed as a convex function in $\boldsymbol{\theta}$. Specifically, if we let $q(\mathbf{x}_{0:K}) \triangleq p(\mathbf{x}_{0:K} | \mathbf{y}_{0:K}, \boldsymbol{\theta}^{(i)})$, the RHS upper bound in (9) can be written as

$$\mathcal{L}(\boldsymbol{\theta}) \lesssim \int p(\mathbf{x}_{0:K} | \mathbf{y}_{0:K}, \boldsymbol{\theta}^{(i)}) \log p(\mathbf{y}_{0:K}, \mathbf{x}_{0:K} | \boldsymbol{\theta}) d\mathbf{x}_{0:K} \quad (10a)$$

$$\simeq \mathcal{Q}(\boldsymbol{\theta}, \boldsymbol{\theta}^{(i)}). \quad (10b)$$

Consider a case where: **(A1)** the motion model is linear; **(A2)** only the process noise covariance matrix is parameter dependent; **(A3)** this process noise is symmetric positive definite, block structured, and linear in the parameters, as

$$\mathbf{Q}_k(\boldsymbol{\theta})^{-1} = \mathbf{M}_k^{(0)} + \sum_{j=1}^{\dim(\boldsymbol{\theta})} \mathbf{M}_k^{(j)} [\boldsymbol{\theta}]_j, \quad (11)$$

with $\{\mathbf{M}_k^{(j)}\}_{j=0}^{\dim(\boldsymbol{\theta})}$ of appropriate dimensions. Assume that (A4) the bases $\mathbf{M}_k^{(j)}$ are block diagonal, each containing a single block $\mathbf{N}_k^{(j)} \in \mathbb{R}^{n_k^j \times n_k^j}$ that is positive definite. The solution minimizing the bound in (10b),

$$\boldsymbol{\theta}_\circ^{(i)} = \operatorname{argmin}_{\boldsymbol{\theta}} \mathcal{Q}(\boldsymbol{\theta}, \boldsymbol{\theta}^{(i)}), \quad (12)$$

can be written compactly as

$$[\boldsymbol{\theta}_\circ^{(i)}]_j = \frac{\sum_{k=0}^{K-1} n_k^j}{\sum_{k=0}^{K-1} \operatorname{Tr}[\mathbf{M}_k^{(j)}(\boldsymbol{\Psi}_k - \boldsymbol{\Gamma}_k \mathbf{A}_k^\top - \mathbf{A}_k \boldsymbol{\Gamma}_k^\top + \mathbf{A}_k \boldsymbol{\Phi}_k \mathbf{A}_k^\top)]},$$

where $\boldsymbol{\Psi}_k, \boldsymbol{\Gamma}_k, \boldsymbol{\Phi}_k$ are computed from the smoothing posterior evaluated with respect to the parameters $\boldsymbol{\theta}^{(i)}$, as

$$\boldsymbol{\Psi}_k = \boldsymbol{\Sigma}_{k+1}^s + \mathbf{m}_{k+1}^s (\mathbf{m}_{k+1}^s)^\top, \quad (13a)$$

$$\boldsymbol{\Gamma}_k = \boldsymbol{\Sigma}_{k+1}^s (\mathbf{G}_k^s)^\top + \mathbf{m}_{k+1}^s (\mathbf{m}_k^s)^\top, \quad (13b)$$

$$\boldsymbol{\Phi}_k = \boldsymbol{\Sigma}_k^s + \mathbf{m}_k^s (\mathbf{m}_k^s)^\top. \quad (13c)$$

Hence, forming and minimizing $\mathcal{Q}(\boldsymbol{\theta}, \boldsymbol{\theta}^{(i)})$ is much faster than computing the two RTS passes, and does not require any costly moment approximations or gradient evaluations once a smoothing posterior has been computed. An EM that alternates between computing the smoothing posterior (E -step), and minimizing \mathcal{Q} (M -step) using (13) given (A1)-(A4) is referred to as a structured EM-algorithm.

3. MODELING

To define the prediction models, we consider two models: a constant position (CP) model with unit variance, with a sampling period of h_k , where $x_{k+1}^{\text{CP}} = x_k^{\text{CP}} + q_k^{\text{CP}}$, $q_k^{\text{CP}} \sim \mathcal{N}(0, h_k)$; and constant velocity (CV) model with, $\mathbf{x}_{k+1}^{\text{CV}} = \mathbf{A}_k^{\text{CV}} \mathbf{x}_k^{\text{CV}} + \mathbf{q}_k^{\text{CV}}$, $\mathbf{q}_k^{\text{CV}} \sim \mathcal{N}(0, (\mathbf{M}_k^{\text{CV}})^{-1})$, and where

$$\mathbf{A}_k^{\text{CV}} \triangleq \begin{bmatrix} \mathbf{I} & h_k \mathbf{I} \\ \mathbf{0} & \mathbf{I} \end{bmatrix}, \quad \mathbf{M}_k^{\text{CV}} \triangleq \frac{12}{h_k^3} \begin{bmatrix} 1 & -\frac{h_k}{2} \\ -\frac{h_k}{2} & \frac{h_k^2}{3} \end{bmatrix}. \quad (14)$$

The reason for these definitions is to simplify the model building and facilitate the EM algorithm. We can now define a receiver model with three-dimensional position $(p^X, p^Y, p^Z) \in \mathbb{R}^3$, where the horizontal positions and lateral velocity $\dot{p}^Z = v^Z \in \mathbb{R}$ are driven by a random walk processes. We collect $\mathbf{z}_k \triangleq (p^X, p^Y, p^Z, v^Z) \in \mathbb{R}^4$, where

$$\mathbf{z}_k = \mathbf{A}_k^z \mathbf{z}_k + \mathbf{q}_k^z, \quad \mathbf{q}_k^z \sim \mathcal{N}(\mathbf{q}_k^z; \mathbf{0}, \mathbf{Q}_k^z(\boldsymbol{\theta})), \quad (15a)$$

$$\mathbf{A}_k^z = \operatorname{diag}(1, 1, \mathbf{A}_k^{\text{CV}}), \quad (15b)$$

$$\mathbf{Q}_k^z(\boldsymbol{\theta})^{-1} = \operatorname{diag}([\boldsymbol{\theta}]_1 h_k^{-1}, [\boldsymbol{\theta}]_2 h_k^{-1}, [\boldsymbol{\theta}]_3 \mathbf{M}_k^{\text{CV}}), \quad (15c)$$

where the parameters $[\boldsymbol{\theta}]_i$ constituting $\boldsymbol{\theta}$ are the inverse variances of the underlying random walks, and linear in a matrix basis parametrizing the inverse process noise covariance. Similarly, we let the ambiguities in the model, $\mathbf{n}_k \in \mathbb{Z}^n$, be driven by an integer random walk. Furthermore, we consider real-valued biases collected in $\boldsymbol{\xi}_k$ (to be defined in Sec. 3.1) driven by random walks in the velocities. Here we consider N_ξ different kinds of biases (ionospheric, tropospheric, etc.), and n relates to the number of visible satellites, N_s , such that $\boldsymbol{\xi}_k \in \mathbb{R}^{N_\xi N_s}$. Hence,

$$\boldsymbol{\xi}_{k+1} = \mathbf{A}_k^\xi \boldsymbol{\xi}_k + \mathbf{q}_k^\xi, \quad \mathbf{q}_k^\xi \sim \mathcal{N}(\mathbf{q}_k^\xi; \mathbf{0}, \mathbf{Q}_k^\xi(\boldsymbol{\theta})), \quad (16a)$$

$$\mathbf{A}_k^\xi = \operatorname{diag}(\mathbf{A}_k^{\text{CV}}, \dots, \mathbf{A}_k^{\text{CV}}) \otimes \mathbf{I}_{N_s}, \quad (16b)$$

$$\mathbf{Q}_k^\xi(\boldsymbol{\theta})^{-1} = \operatorname{diag}([\boldsymbol{\theta}]_{3+1} \mathbf{M}_k^{\text{CV}}, \dots, [\boldsymbol{\theta}]_{3+N_\xi} \mathbf{M}_k^{\text{CV}}) \otimes \mathbf{I}_{N_s}. \quad (16c)$$

We reorder the states $\mathbf{x}_k \triangleq (\mathbf{z}_k; \mathbf{n}_k; \boldsymbol{\xi}_k)$, obtaining

$$\mathbf{x}_{k+1} = \underbrace{\begin{bmatrix} \mathbf{A}_k^z & \mathbf{0} & \mathbf{0} \\ \mathbf{0} & \mathbf{I} & \mathbf{0} \\ \mathbf{0} & \mathbf{0} & \mathbf{A}_k^\xi \end{bmatrix}}_{\triangleq \mathbf{A}_k} \mathbf{x}_k + \underbrace{\begin{bmatrix} \mathbf{I} & \mathbf{0} \\ \mathbf{0} & \mathbf{0} \\ \mathbf{0} & \mathbf{I} \end{bmatrix}}_{\triangleq \mathbf{B}_k^{\mathbb{R}}} \mathbf{q}_k + \underbrace{\begin{bmatrix} \mathbf{0} \\ \mathbf{I} \\ \mathbf{0} \end{bmatrix}}_{\triangleq \mathbf{B}_k^z} \mathbf{s}_k, \quad (17a)$$

in the form of (1a) which satisfies (A1)-(A4), with

$$\mathbf{Q}_k^{\mathbb{R}}(\boldsymbol{\theta}) = \operatorname{diag}(\mathbf{Q}_k^z(\boldsymbol{\theta}), \mathbf{Q}_k^\xi(\boldsymbol{\theta})). \quad (17b)$$

This is a flexible model that will be defined differently depending on the considered GNSS measurement model.

3.1 GNSS Measurement Models

In this section, we consider the classic GNSS measurements provided in the RINEX format. Here, \mathcal{R} denotes a receiver, \mathcal{B} denotes a base station, and $s \in \mathbb{N}_{>0}$ denotes a satellite. The measurements include a pseudo-range $P_{\mathcal{R}}^s \in \mathbb{R}$ computed by an auto-correlation on the pseudo-random code, the phase-range $\Phi_{\mathcal{R}}^s \in \mathbb{R}$ containing the integer ambiguity, and a Doppler measurement $\Gamma_{\mathcal{R}}^s \in \mathbb{R}$. Fig. 1 provides the equations, defined in signals summarized in Table 1. Here, the functional dependency indicates channels on which the signal differs. For instance, the noise $\epsilon_{\mathcal{R}}^s$ between a satellite and receiver is realized differently on every combination of measurements $\{P, \Phi, \Gamma\}$ with a unique frequency band L_j . On the other hand, the initial oscillator phases only depend on the frequency band L_j , as they solely appear in the phase-range measurements.

Table 1. Summary of GNSS model parameters.

Variable	Functional dep.	Description
$\rho_{\mathcal{R}}^s$	-	Euclidean distance from \mathcal{R} to s
$dt_{\mathcal{R}}, dt^s$	-	Clock offset
$D_{\mathcal{R}}, D^s$	L_j and $\{P, \Phi\}$	Inter-frequency bias
N	L_j	Integer ambiguity bias
λ_j	L_j	(= f_j^{-1}) Carrier wavelength
f_j	L_j	(= λ_j^{-1}) Carrier frequency
α_c^d	L_c, L_d	(= f_d^2 / f_c^2) ionosphere-free const.
$T_{\mathcal{R}}^s$	-	Tropospheric delay
$I_{\mathcal{R}}^s$	L_j	Ionospheric delay
$M_{\mathcal{R}}^s$	L_j and $\{P, \Phi\}$	Multipath effects
$\epsilon_{\mathcal{R}}^s$	L_j and $\{P, \Phi, \Gamma\}$	Gaussian noise

To proceed, we define three different ways of combining the GNSS measurements, which are often used in practice to reduce the impact of the various biases in Fig. 1.

Definition 1. Let g represent any signal in Table 1, then

- A Single Difference (SD), is defined as

$$\Delta^{ab}(g_i^s(L_j)) \triangleq g_i^s(L_j)|_{s=a} - g_i^s(L_j)|_{s=b};$$

- A Base-Receiver Difference (BRD), is defined as

$$\nabla_{\mathcal{RB}}(g_i^s(L_j)) \triangleq g_i^s(L_j)|_{i=\mathcal{R}} - g_i^s(L_j)|_{i=\mathcal{B}};$$

- A Double Difference (DD), is defined with as

$$\nabla \Delta_{\mathcal{RB}}^{ab}(g_i^s(L_j)) \triangleq \Delta^{ab}(\nabla_{\mathcal{RB}}(g_i^s(L_j)))$$

- An Ionosphere-Free (IF) combination, is defined as

$$\text{IF}_c^d(g(L_j)) \triangleq g(L_j) - \alpha_c^d g(L_d).$$

The appeal of working with measurements subjected to the DD operation, which not only includes measurements from a receiver (\mathcal{R}) but also measurements from a base station (\mathcal{B}), is that clock drift biases and inter-frequency biases

$P_i^s(L_j) = +\rho_i^s + c[dt_i - dt^s] + [D_i(L_j, P) - D^s(L_j, P)] + T_i^s + I_i^s(L_j) + M_i^s(L_j, P) + \epsilon_i^s(L_j, P)$
$\Phi_i^s(L_j) = +\rho_i^s + c[dt_i - dt^s] + [D_i(L_j, \Phi) - D^s(L_j, \Phi)] + T_i^s - I_i^s(L_j) + M_i^s(L_j, \Phi) + \lambda_j N_i(L_j) + \epsilon_i^s(L_j, \Phi)$
$\Gamma_i^s(L_j) = -\dot{\rho}_i^s - c[\dot{dt}_i - \dot{dt}^s] - \dot{T}_i^s + \dot{I}_i^s(L_j) - \dot{M}_i^s(L_j, \Phi) + \epsilon_i^s(L_j, \Gamma)$

Fig. 1. GNSS observation equations for a receiver i and a specific satellite $s \in [1, N_s]$ over frequency the bands $\{L_j\}$.

disappear from the estimation problem. Additionally, if there exist astrophysical models of the ionospheric and tropospheric biases, the resulting estimator becomes less sensitive to modeling errors (as will be discussed later). To proceed, we permit the SD-, DD-, and IF-maps to operate on vectors. Without loss of generality, we let the satellite $s = 1$ be the positive satellite in any differencing scheme.

Definition 2. Consider a vector $\mathbf{g}_i^s(L_j)$, with elements $[g_i^s(L_j)]_l = g_i^s(L_j)$ being any signal in Table 1. Let

$$\begin{aligned} \bar{\Delta} : \mathbb{R}^{N_s} &\mapsto \mathbb{R}^{N_s-1} & [\bar{\Delta}(\mathbf{g})]_{l-1} &= \Delta^{1,l}(g_i^s(L_j)) \\ \bar{\nabla} : \mathbb{R}^{N_s} &\mapsto \mathbb{R}^{N_s} & [\bar{\nabla}(\mathbf{g})]_{l-1} &= \nabla_{\mathcal{R}\mathcal{B}}(g_i^s(L_j)) \\ \overline{\nabla\Delta} : \mathbb{R}^{N_s} \times \mathbb{R}^{N_s} &\mapsto \mathbb{R}^{N_s-1} & [\overline{\nabla\Delta}(\mathbf{g})]_{l-1} &= \Delta^{1,l}(g_i^s(L_j)) \\ \overline{\text{IF}}_c^d : \mathbb{R}^{N_s} \times \mathbb{R}^{N_s} &\mapsto \mathbb{R}^{N_s} & [\overline{\text{IF}}_c^d(\mathbf{g})]_{l-1} &= \text{IF}_c^d(g_i^s(L_j)) \end{aligned}$$

3.2 A DD+IF Multi-band Measurement Model

In this measurement model, we consider three frequency bands and two vector-valued bias states evolving by the CV model in (16). The integer ambiguities are double differenced, and the measurement model is defined by

$$\mathbf{y}_k \triangleq \begin{bmatrix} \overline{\nabla\Delta}(\mathbf{P}_k(L_1)) \\ \overline{\nabla\Delta}(\Phi_k(L_1)) \\ \overline{\nabla\Delta}(\Gamma_k(L_1)) \\ \overline{\text{IF}}_1^2(\overline{\nabla\Delta}(\mathbf{P}_k(L_j))) \\ \overline{\text{IF}}_1^2(\overline{\nabla\Delta}(\Phi_k(L_j))) \\ \overline{\text{IF}}_1^2(\overline{\nabla\Delta}(\Gamma_k(L_j))) \\ \overline{\text{IF}}_1^3(\overline{\nabla\Delta}(\mathbf{P}_k(L_j))) \\ \overline{\text{IF}}_1^3(\overline{\nabla\Delta}(\Phi_k(L_j))) \\ \overline{\text{IF}}_1^3(\overline{\nabla\Delta}(\Gamma_k(L_j))) \\ \overline{\nabla}(\mathbf{I}_k(L_1)) \\ \overline{\nabla}(\mathbf{T}_k) \end{bmatrix}, \quad \mathbf{n}_k \triangleq \begin{bmatrix} \overline{\nabla\Delta}(\mathbf{N}_k(L_1)) \\ \overline{\nabla\Delta}(\mathbf{N}_k(L_2)) \\ \overline{\nabla\Delta}(\mathbf{N}_k(L_3)) \end{bmatrix}, \quad \boldsymbol{\xi}_k \triangleq \begin{bmatrix} \overline{\nabla}(\mathbf{I}_k(L_1)) \\ \overline{\nabla}(\frac{d}{dt}\mathbf{I}_k(L_1)) \\ \overline{\nabla}(\mathbf{T}_k) \\ \overline{\nabla}(\frac{d}{dt}\mathbf{T}_k) \end{bmatrix}. \quad (18)$$

including virtual measurements on the BRD-bias terms from physical models, such as the Klobuchar and SBAS models, see Tian et al. (2022). The reason for including these models in the measurement equation is to allow deviations from the deterministic bias models, which enables us to reason about how uncertainty in the bias models affect the quality of the estimates. Here, the resulting model is observable, and the measurement model is nonlinear in \mathbf{z}_k , but linear in $\{\mathbf{n}_k, \boldsymbol{\xi}_k\}$. The maps \mathbf{g}_k and $\{\mathbf{C}_k, \mathbf{R}_k\}$ in (6) follow directly from Fig. 1 and Definitions 1-2.

3.3 A SD+IF Multi-band Measurement Model

In this model, every instance of the DD- and SD-operation in (18) is replaced by SD- and undifferenced signals, respectively. Furthermore, the state vector is extended with the satellite clock biases $\mathbf{dt} = (dt_k^1, \dots, dt_k^{N_s}) \in \mathbb{R}^{N_s}$, and these obey a CV model. Here, we once again include virtual measurements of the biases from physical models, but also include a measurement on the clock bias of the positive satellite dt_k^1 to make the entire estimation model observable. The reason for defining the problem in this way is that it permits an extension to a multi-agent setting, where several agents model the same satellite clock offsets.

4. AN ADAPTIVE POST-PROCESSING ALGORITHM

In this section, we define the proposed Adaptive Post-Processing (APP) algorithm in three steps. We start by discussing the notion of adaptive ambiguity priors in Sec. 4.1, which is used to define an RTS-smoother with adaptive priors (RTSAP). This algorithm fixes the inverse basis of the process noise based on a 1-step ahead filtering innovation error. Next, we discuss the heuristics used to approximately solve the NP-hard integer fixation problem in Sec. 4.2, defining a unimodular de-correlating transform (UDT) and an integer search method (ISM). Finally, the APP-algorithm is defined using structured EM in Sec. 4.3.

4.1 Relaxed Smoothing with Adaptive Ambiguity Priors

In the smoothing, we first consider a relaxed estimation problem, where the ambiguities evolve by a random walk over the real numbers. However, to capture the sporadic jumps that these ambiguities exhibit, the process noise is adapted depending on if a cycle-slip is likely to have occurred. The presence or absence of a cycle-slip is determined by comparing the 1-step measurement prediction with the actual measurement, ascribing all of the variation in the prediction error to individual ambiguity dimensions,

$$\bar{\mathbf{n}}_{k-1} \triangleq |(\mathbf{G}_k^\top \mathbf{G}_k)^{-1} \mathbf{G}_k^\top (\mathbf{y}_k - \mathbf{m}_{k|k-1}^y)|, \quad (19a)$$

$$\mathbf{G}_k \triangleq \frac{\partial}{\partial \mathbf{x}_k^{\mathbb{Z}}} (\mathbf{h}(\mathbf{x}_k) + \mathbf{C}_k \mathbf{x}_k) \Big|_{\mathbf{x}_k = \mathbf{m}_{k|k-1}}, \quad (19b)$$

and determining the presence or absence of a cycle-slip between a time $k-1$ and k by applying a threshold to this value, here denoted by ϵ_{amb} ambiguities. Consequently, in the filtering the process noise is

$$\mathbf{Q}_k(\boldsymbol{\theta}) = \mathbf{B}_k^q \mathbf{Q}_k^{\mathbb{R}}(\boldsymbol{\theta}) (\mathbf{B}_k^q)^\top + \mathbf{B}_k^z \mathbf{Q}_k^{\mathbb{Z}} (\mathbf{B}_k^z)^\top, \quad (20a)$$

$$\mathbf{Q}_k^{\mathbb{Z}} = (\sigma_L^2) \mathbf{I} + (\sigma_H^2 - \sigma_L^2) \text{diag}(\mathbf{o}_k), \quad (20b)$$

$$[\mathbf{o}_k]_i = \begin{cases} 1 & \text{if } [\bar{\mathbf{n}}_k]_i > \epsilon_{\text{amb}} \\ 0 & \text{otherwise} \end{cases}, \quad (20c)$$

which is the same approach as in Greiff et al. (2021). When performing RTS smoothing adaptive ambiguity prior, we compute the sequence $\mathbf{Q}_{0:K-1}(\boldsymbol{\theta})$ in the forward pass, as described in (19a) and summarized in Algorithm 1.

4.2 Integer Fixation Heuristics

Having computed a relaxed posterior $p(\mathbf{x}_k | \mathbf{y}_{0:K}, \boldsymbol{\theta})$ using the relaxed estimation model (letting $\mathbf{x} \in \mathbb{R}^{m+n}$ and using the adapted process noise), we subsequently fix the ambiguities using methods common to GNSS positioning. Specifically, we compute a unimodular decorrelating transform (UDT) as $\mathbf{Z}_k \in \mathbb{Z}^{n \times n}$ based on $p(\mathbf{x}_k^{\mathbb{Z}} | \mathbf{y}_{0:K}, \boldsymbol{\theta}) = \mathcal{N}(\mathbf{x}_k^{\mathbb{Z}}, \mathbf{m}_k^{\mathbb{Z}}, \boldsymbol{\Sigma}_k^{\mathbb{Z}})$, which aspires to find a transformed $\boldsymbol{\eta}_k \in \mathbb{Z}^n$ where $\mathbf{Z}_k \boldsymbol{\Sigma}_k^{\mathbb{Z}} \mathbf{Z}_k^\top$ is less correlated than $\boldsymbol{\Sigma}_k^{\mathbb{Z}}$. To this end, we use the M-LAMBDA method in Chang et al. (2005).

In the decorrelated ambiguity space, we find the most likely ambiguity hypothesis by solving the ML-problem

Algorithm 1 Nonlinear RTS smoother with Adaptive Ambiguity Prior (RTSAP) computed in the forward pass.

```

1: Receive:  $\mathbf{y}_{0:K}, \mathbf{m}_0, \mathbf{P}_0, \mathbf{A}_{0:K-1}, \mathbf{h}_{0:K}, \mathbf{R}_{0:K}, \sigma_L, \sigma_H, \boldsymbol{\theta}$ 
2: for  $k = 1, 2, \dots, K$  do
3:   Compute  $\mathbf{o}_{k-1}$  from  $\{\mathbf{y}_k, \mathbf{m}_{k-1}\}$  by (19a)
4:    $\{\mathbf{M}_{k-1}^{(j)}\}_{j=0}^{\dim(\boldsymbol{\theta})} \leftarrow \text{get\_basis}(\mathbf{o}_{k-1}, \sigma_L, \sigma_H)$  by (20)
5:    $\{\mathbf{m}_k, \boldsymbol{\Sigma}_k\} \leftarrow \text{KF}(\mathbf{m}_{k-1}, \boldsymbol{\Sigma}_{k-1}, \mathbf{y}_k, \boldsymbol{\theta})$  using any
     method in Sec. 2.2 for the nonlinearity.
6: end for
7: Initialize  $\mathbf{m}_K^s = \mathbf{m}_K, \boldsymbol{\Sigma}_K^s = \boldsymbol{\Sigma}_K$ 
8: for  $k = K-1, \dots, 0$  do
9:    $\{\mathbf{m}_k^s, \mathbf{P}_k^s, \mathbf{G}_k^s\} \leftarrow \text{BP}(\mathbf{m}_{k+1}^s, \boldsymbol{\Sigma}_{k+1}^s, \mathbf{G}_{k+1}^s, \mathbf{m}_k, \dots,$ 
      $\boldsymbol{\Sigma}_k, \mathbf{m}_{k|k+1}, \boldsymbol{\Sigma}_{k|k+1}, \mathbf{A}_k)$  by (4)
10: end for
11: Output:  $\{\mathbf{m}_k, \boldsymbol{\Sigma}_k, \mathbf{m}_k^s, \boldsymbol{\Sigma}_k^s\}_{k=0}^K, \{\mathbf{M}_k^{(j)}\}_{k=0, j=0}^{k=K-1, j=\dim(\boldsymbol{\theta})}$ 

```

$$\boldsymbol{\eta}_k^I = \underset{\boldsymbol{\eta}_k^I \in \mathbb{Z}^m}{\text{argmin}} \|\boldsymbol{\eta}_k^I - \mathbf{Z}_k \mathbf{m}_k^{\mathbb{Z}}\|_{(\mathbf{Z}_k \boldsymbol{\Sigma}_k^{\mathbb{Z}} \mathbf{Z}_k^{\top})^{-1}}, \quad (21)$$

approximately using a simple boot-strapping method (refer to Teunissen (2001)), before converting this into the original ambiguity space $\mathbf{n}_k^I = \mathbf{Z}_k^{-1} \boldsymbol{\eta}_k^I \in \mathbb{Z}^n$. This is referred to as an Integer Search Method (ISM). In the implementation, the integer fixation is done independently at each time-step, as done in the cited filtering methods. Note that the *integer fixation density* used in (21) can also be taken as the filtering posterior $p(\mathbf{x}_k | \mathbf{y}_{0:k}, \boldsymbol{\theta})$. A comparison of fixing the integer on the smoothing versus the filtering posterior is provided in Sec. 5.1.

4.3 Full Post-Processing Algorithm

We are now ready to express the full adaptive post-processing algorithm (APP). We first perform a two-way pass with the RTSAP in Algorithm 1 of the relaxed dynamics (letting $\mathbf{x}_k \in \mathbb{R}^{n+m}$), where the cycle-slip detection is used to form the matrix-basis of the inverse process noise $\{\mathbf{M}_k^{(j)}\}_{k,j}$. Next, we iterate the M -steps and E -steps in the structured EM algorithm defined in Sec. 2.3, to optimize the parameters $\boldsymbol{\theta}$ given $\{\mathbf{M}_k^{(j)}\}_{k,j}$ and $\mathbf{y}_{0:K}$. This is done until the majorizing objective satisfies $\mathcal{Q}(\boldsymbol{\theta}^{(i-1)}, \boldsymbol{\theta}^{(i-2)}) - \mathcal{Q}(\boldsymbol{\theta}^{(i)}, \boldsymbol{\theta}^{(i-1)}) \leq \epsilon_{\text{tol}}$, or until reaching a maximum number of N_{max} iterations. Based on the smoothing posterior from the last EM-iteration, the integer trajectory is subsequently fixed using the fixation outlined in Sec. 4.2, and we finally compute a fixed estimate $p(\mathbf{x}_k^{\mathbb{R}} | \mathbf{n}_{0:K}^I, \mathbf{y}_{0:K}, \boldsymbol{\theta}^{(*)}) \approx \mathcal{N}(\mathbf{x}_k^{\mathbb{R}}; \check{\mathbf{m}}_k^s, \check{\boldsymbol{\Sigma}}_k^s)$ using any RTS smoother in Sec. 2, outputting $\check{\mathbf{m}}_k^s, \check{\boldsymbol{\Sigma}}_k^s, \mathbf{n}_{0:K}^I$. This adaptive post-processing is sketched in Algorithm 2.

5. NUMERICAL EXAMPLES

To demonstrate the algorithms, we present a quantitative study to assess the choice of measurement equation, fixation density, and moment approximation scheme on the estimation performance of the RTSAP. This serves as the benchmark for the subsequent simulation study of the adaptive post-processing scheme APP, in which the measurement noise covariance is initialized erroneously. The parameters for the study are given in Appendix A.

5.1 Simulation Study of the RTASP with known parameters

We start by considering the RTSAP defined in Algorithm 1 in a setting where the noise statistics are known perfectly.

Algorithm 2 Pseudo-code for the Adaptive GNSS Post-Processing (APP) with EM and adaptive ambiguity priors.

```

1: Initialize:  $\mathbf{m}_0, \boldsymbol{\Sigma}_0, \boldsymbol{\theta}^{(0)}, \mathbf{y}_{0:K}, i = 1.$ 
2:  $\{\mathbf{m}_k, \mathbf{P}_k, \mathbf{m}_k^s, \mathbf{P}_k^s, \mathbf{G}_k^s, \mathbf{M}_k\}_{k=0}^K \leftarrow \text{RTSAP}(\mathbf{y}_{0:K}, \boldsymbol{\theta}^{(0)})$ 
   using the RTS with adaptive prior in Algorithm 1
3: while  $i \leq N_{\text{max}}$  and EM has not converged do
4:    $\boldsymbol{\theta}^{(i)} \leftarrow \underset{\boldsymbol{\theta} \in D_{\boldsymbol{\theta}}}{\text{argmin}} \mathcal{Q}(\boldsymbol{\theta}; \boldsymbol{\theta}^{(i-1)})$  using (13)
5:   Define  $\mathbf{Q}_{0:K}^{(i)}$  using the basis  $\mathbf{M}_{0:K}$  and  $\boldsymbol{\theta}^{(i)}$ 
6:    $\{\mathbf{m}_k, \boldsymbol{\Sigma}_k, \mathbf{m}_k^s, \mathbf{P}_k^s, \mathbf{G}_k^s\}_{k=0}^K \leftarrow \text{RTS}(\mathbf{y}_{0:K}, \mathbf{Q}_{0:K}^{(i)})$ 
     using any of the RTS smoothers in Sec. 2
7: end while
8: for  $k = 0, \dots, K$  do
9:    $\mathbf{Z}_k \leftarrow \text{UDT}(p(\mathbf{n}_k | \mathbf{y}_{0:K}, \boldsymbol{\theta}^{(*)}))$ 
10:   $\mathbf{n}_k^I \leftarrow \text{ISM}(p(\mathbf{n}_k | \mathbf{y}_{0:K}, \boldsymbol{\theta}^{(*)}), \mathbf{Z}_k)$ 
11: end for
12:  $\{\check{\mathbf{m}}_k, \check{\boldsymbol{\Sigma}}_k, \check{\mathbf{m}}_k^s, \check{\boldsymbol{\Sigma}}_k^s, \check{\mathbf{G}}_k^s\}_{k=0}^K \leftarrow \text{RTS}(\mathbf{y}_{0:K}, \mathbf{n}_{0:K}^I, \mathbf{Q}_{0:K}^{(i)})$ 
   using any of the RTS smoothers in Sec. 2
13: Return,  $\check{\mathbf{m}}_{0:K}^s, \check{\boldsymbol{\Sigma}}_{0:K}^s, \mathbf{n}_{0:K}^I, \boldsymbol{\theta}^{(*)}$ 

```

This is done to: (i) ensure that the filter/smoothing posteriors are consistent with the empirical statistics, even though an approximate integer fixation scheme is used; (ii) study the impact of fixing the ambiguities (see Sec. 4.2) on the filtering/smoothing posteriors; and (iii) assess how the use of various moment approximations affect performance in this setting. To this end, we conduct a Monte-Carlo (MC) simulation study with $N_{\text{MC}} = 10^3$ different realizations of the errors and noise for 12 permutations of the RTASP:

- (i) DD-IF/SD-IF measurement models;
- (ii) Integer fixation on the filtering/smoothing posteriors;
- (iii) The ERTS/UT-PL-RTS/SR-PL-RTS approximations.

To assess consistency, we define the following statistics:

- The positional root mean-square error (RMSE)

$$\text{RMSE}_k(\mathbf{p}) \triangleq \left(\frac{1}{N_{\text{MC}}} \sum_{n=1}^{N_{\text{MC}}} \|\boldsymbol{\Pi}(\mathbf{x}_k^{\mathbb{R},(n)} - \check{\mathbf{m}}_k^{(n)})\|_2^2 \right)^{1/2}, \quad (22)$$

where $\boldsymbol{\Pi}$ extracts the positional subset of $\mathbf{x}_k^{\mathbb{R}}$, and the superscript $(\cdot)^{(n)}$ denotes the n th simulation.

- The root positional posterior covariance (RAPC),

$$\text{RAPC}_k(\mathbf{p}) \triangleq \left(\frac{1}{N_{\text{MC}}} \sum_{n=1}^{N_{\text{MC}}} \text{Tr}[\boldsymbol{\Pi} \check{\boldsymbol{\Sigma}}_k^{(n)} \boldsymbol{\Pi}^{\top}] \right)^{1/2}. \quad (23)$$

When using the PL-SR-RTS, the resulting statistics are plotted in Fig. 2. Here, we note that the fixed estimate errors of the RTSAP does seem to be consistent with the variance estimates. We observe a slight difference in performance when using the SD-IF and DD-IF models, with the former yielding a lower positional RMSE. However, as the difference is very slight, we recommend using the DD-IF in practice, as it is less sensitive to errors in the deterministic bias models. Finally, we note a significant difference between the fixed estimates computed with respect to the filtering and smoothing posteriors, with the estimates fixed on the filtering posterior (red/black) resulting in a positional RMSE almost 30% higher than the fixed estimates computed from the smoothing posterior (blue/green). Furthermore, we note a much faster transient in the positional errors when fixed on the smoothing poste-

Table 2. Summary of quantitative results from 10^3 MC runs for permutations of the Algorithm 1.

Model	Fixation density	Scheme	TA-RMSE (\downarrow)	S-RMSE [m] (\downarrow)	S-RAPC [m] (\downarrow)	TA-IFA [%] (\uparrow)	CT [s] (\downarrow)
DD-IF	Filtering	ERTS	$3.056 \cdot 10^{-1}$	$5.422 \cdot 10^{-2}$	$5.499 \cdot 10^{-2}$	97.675	4.725
DD-IF	Filtering	UT-PL-RTS	$3.056 \cdot 10^{-1}$	$5.422 \cdot 10^{-2}$	$5.499 \cdot 10^{-2}$	97.675	6.272
DD-IF	Filtering	SR-PL-RTS	$3.056 \cdot 10^{-1}$	$5.422 \cdot 10^{-2}$	$5.499 \cdot 10^{-2}$	97.675	6.350
DD-IF	Smoothing	ERTS	$4.732 \cdot 10^{-2}$	$3.838 \cdot 10^{-2}$	$4.063 \cdot 10^{-2}$	99.843	4.877
DD-IF	Smoothing	UT-PL-RTS	$4.732 \cdot 10^{-2}$	$3.838 \cdot 10^{-2}$	$4.063 \cdot 10^{-2}$	99.843	6.230
DD-IF	Smoothing	SR-PL-RTS	$4.732 \cdot 10^{-2}$	$3.838 \cdot 10^{-2}$	$4.063 \cdot 10^{-2}$	99.843	6.245
SD-IF	Filtering	ERTS	$2.789 \cdot 10^{-1}$	$4.655 \cdot 10^{-2}$	$5.379 \cdot 10^{-2}$	98.507	6.248
SD-IF	Filtering	UT-PL-RTS	$2.789 \cdot 10^{-1}$	$4.655 \cdot 10^{-2}$	$5.379 \cdot 10^{-2}$	98.507	7.672
SD-IF	Filtering	SR-PL-RTS	$2.789 \cdot 10^{-1}$	$4.655 \cdot 10^{-2}$	$5.379 \cdot 10^{-2}$	98.507	7.574
SD-IF	Smoothing	ERTS	$4.021 \cdot 10^{-2}$	$3.848 \cdot 10^{-2}$	$3.970 \cdot 10^{-2}$	99.899	6.057
SD-IF	Smoothing	UT-PL-RTS	$4.021 \cdot 10^{-2}$	$3.848 \cdot 10^{-2}$	$3.970 \cdot 10^{-2}$	99.899	7.433
SD-IF	Smoothing	SR-PL-RTS	$4.021 \cdot 10^{-2}$	$3.848 \cdot 10^{-2}$	$3.970 \cdot 10^{-2}$	99.899	7.364

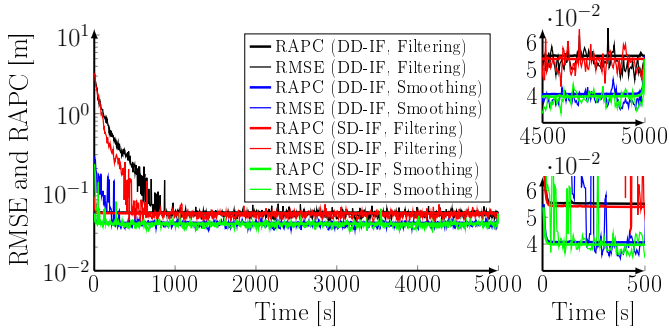


Fig. 2. Positional RMSE and RAPC in time, indicating that the fixed estimates are consistent after the initial transient where the ambiguities are incorrectly fixed.

rior. Here, the utilization of future measurements greatly reduces the initial uncertainty in the relaxed estimates, thereby improving the fixed estimate convergence time.

To get more insight on this, we consider the following:

- Time-averaged RMSE, as $\frac{1}{K+1} \sum_{k=0}^K \text{RMSE}_k(\mathbf{p})$;
- Stationary RMSE, defined as $\text{RMSE}_{k=K/2}(\mathbf{p})$;
- Stationary RAPC, defined as $\text{RAPC}_{k=K/2}(\mathbf{p})$;
- Time-averaged integer fixation accuracy (TA-IFA), as the percentage of correctly fixed ambiguities in time considering each dimension of \mathbf{n}_k^I independently;
- Computational time¹ of running the resulting RTSAP.

The statistics are computed for the 12 possible combinations of (i)–(iii) in Table 2, where the variants with the PL-SR-version which was depicted in Fig. 2 are highlighted.

The choice of moment approximation has little impact on performance. Indeed, the statistics only differ after the fourth decimal when varying ERTS/UT-PL-RTS/SR-PL-RTS. We observe the same general performance as indicated by Fig. 2, and also note a significant difference in the time-averaged integer fixation accuracy when using the filter/smoothing posteriors. This largely explains the difference in the time-averaged statistics, where the empirical errors are inflated due to the fixation being poor. We also note that the computational time for running the RTSAP is about 30% greater when using the PL-RTS moment matching schemes. On this basis, it is clear that the choice of DD-IF/SD-IF and ERTS/UT-PL-RTS/SR-PL-RTS matters less than on which density the integers are fixed.

¹ Using Matlab on an 8-core 11th Gen Intel i7-1165G7 @ 2.80GHz.

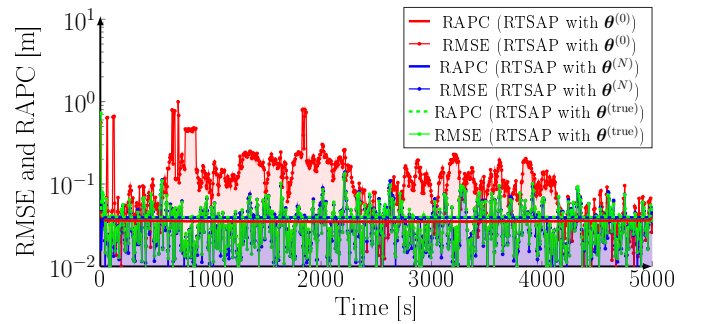


Fig. 3. Positional RMSE and RAPC for: (A) the RTSAP (red) and (B) the APP (blue) with bad parameters; and (C) the RTSAP (green) with perfect parameters.

5.2 Simulation Study of the APP with parameter adaptation

As the estimates are consistent and we see significant improvements when fixing the integer ambiguities on the smoothing posterior, we next provide a second simulation demonstrating the effects of parameter adaptation in the APP. Due to the observations in the quantitative results we consider three ways of computing the estimates:

- The same RTSAP algorithm with the SD-IF model, but with poorly initialized parameters, $\theta^{(0)} \neq \theta^{\text{true}}$.
- A APP post-processing algorithm, run with an ERTS, the SD-IF measurement model, but with the same poorly initialized model parameters, $\theta^{(0)}$ as in (A).
- The RTSAP in Algorithm 1 as in (A), run with an ERTS, the SD-IF measurement model, and knowledge of the true model parameters θ^{true} (as in Sec. 5.1);

Once again, we compute a positional RMSE and RAPC, now from $N_{MC} = 10$ simulations, as shown in Fig. 3, using the ERTS with the SD-IF model and fixing the estimates on the smoothing posterior (the same measures as the green signals as in Fig. 2), and the majorizing objective in the APP is also shown as a function of the EM iterates in Fig 4.

As we know the RAPC to be consistent with the empirical positioning error statistics when the model parameters are known (refer to Sec. 5.1), we note that the RTSAP initialized with the erroneous model parameters greatly overestimates the confidence of the fixed estimates. Indeed, the RAPC in (A) is lower than that in (B) and (C), yet the positioning errors are significantly larger in (A). Here, the adaptation in the APP algorithm yields a significantly better model, and the errors in (B) are much smaller than

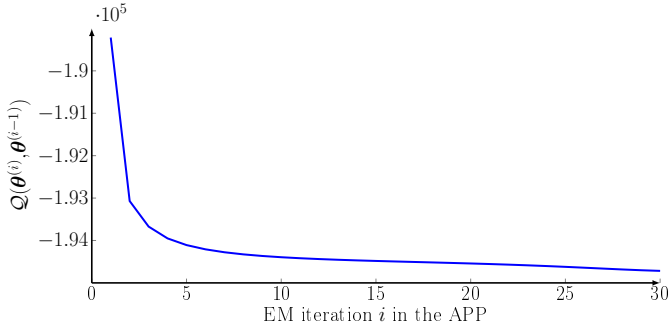


Fig. 4. Convergence of $Q(\boldsymbol{\theta}^{(i)}, \boldsymbol{\theta}^{(i-1)})$ in i for the APP.

that of (A) as a consequence, despite the two algorithms being initialized with the same model parameters.

6. CONCLUSION

In this paper, we explore how fast and efficient smoothing algorithms can be implemented for GNSS post-processing using: (i) two different candidate measurement models; (ii) different ways of fixing the integer ambiguities; and (iii) various RTS smoothers. We demonstrate that due to the largely linear estimation model, the choice of moment approximation scheme or measurement model has a limited effect on the empirical error statistics when the parameters of the estimation model are perfectly known. Instead, the design choice resulting in greatest performance improvement was the density on which the integer ambiguities were fixed. For the considered measurement models and moment approximation schemes, fixing on the smoothing posterior led to a reduction in empirical positional RMSE of approximately 30%. Additionally, fixing the ambiguities on the smoothing posterior significantly improved the convergence time of the positional estimates.

We also demonstrate that parameter adaption, when done in the EM framework, can yield significant improvements in GNSS post-processing when the model parameters are not perfectly known. Here, we propose the adaptive post-processing APP algorithm, which uses the RTSAP on the first EM-iteration to fix the noise covariance basis, subsequently fitting the parameters of the estimation model. Doing so does not achieve a perfect estimate of the model parameters, but significantly improves the position RMSE in the fixed estimates and the integer fixation accuracy.

Future work will evaluate and validate the proposed RTSAP and APP on GNSS experiment logs, and extend the algorithm to a multi-receiver post-processing setting.

REFERENCES

- Arasaratnam, I. (2009). *Cubature Kalman filtering theory & applications*. Ph.D. thesis.
- Berntorp, K., Weiss, A., and Di Cairano, S. (2018). GNSS ambiguity resolution by adaptive mixture Kalman filter. In *IEEE Int. Conf. on Information Fusion*, 1–5.
- Chang, X.W., Yang, X., and Zhou, T. (2005). MLAMBDA: Modified LAMBDA method for integer least-squares estimation. *Journal of Geodesy*, 79(9), 552–565.
- Fraser, D. and Potter, J. (1969). The optimum linear smoother as a combination of two optimum linear filters. *IEEE Trans. on automatic control*, 14(4), 387–390.
- Greiff, M., Berntorp, K., Di Cairano, S., and Kim, K.J. (2021). Mixed-integer linear regression Kalman filters for gnss positioning. In *IEEE Conf. on Control Technology and Applications*, 980–985.
- Greiff, M., Robertsson, A., and Berntorp, K. (2020). Exploiting linear substructure in linear regression Kalman filters. In *IEEE Conf. Decision and Cont.*, 2942–2948.
- Kitagawa, G. (1987). Non-gaussian state-space modeling of nonstationary time series. *Journal of the American statistical association*, 82(400), 1032–1041.
- Leick, A., Rapoport, L., and Tatarnikov, D. (2015). *GPS satellite surveying*. John Wiley & Sons.
- Odolinski, R. and Teunissen, P.J. (2016). Single-frequency, dual-GNSS versus dual-frequency, single-GNSS: a low-cost and high-grade receivers GPS-BDS RTK analysis. *Journal of geodesy*, 90(11), 1255–1278.
- Rauch, H.E., Tung, F., and Striebel, C.T. (1965). Maximum likelihood estimates of linear dynamic systems. *AIAA Journal*, 3(8), 1445–1450.
- Särkkä, S. (2013). *Bayesian filtering and smoothing*, volume 3. Cambridge university press.
- Takasu, T. and Yasuda, A. (2010). Kalman-filter-based integer ambiguity resolution strategy for long-baseline RTK with ionosphere and troposphere estimation. In *ION GNSS*, 161–171.
- Teunissen, P.J. (2001). GNSS ambiguity bootstrapping: theory and application. In *Int. symposium on kinematic systems in Geodesy, geomatics and navigation*, 246–254.
- Teunissen, P. (1997). A canonical theory for short GPS baselines. Part III: the geometry of the ambiguity search space. *Journal of Geodesy*, 71(8), 486–501.
- Teunissen, P., De Jonge, P., and Tiberius, C. (1995). The LAMBDA method for fast GPS surveying. In *Int. Symp. GPS Tech. App.*
- Tian, Y., Li, S., Shen, H., Zhang, W., and Hao, W. (2022). Comparative analysis of BDGIM, NeQuick-G, and Klobuchar ionospheric broadcast models. *Astrophysics and Space Science*, 367(8), 1–14.
- Vaclavovic, P. and Dousa, J. (2015). Backward smoothing for precise GNSS applications. *Adv. in Space Research*, 56(8), 1627–1634.
- Wan, E.A. and Van Der Merwe, R. (2000). The unscented Kalman filter for nonlinear estimation. In *Adaptive Systems for Signal Process., Com., and Control Symp.*
- Zhao, S., Cui, X., Guan, F., and Lu, M. (2014). A Kalman filter-based short baseline RTK algorithm for single-frequency combination of GPS and BDS. *Sensors*, 14(8), 15415–15433.

Appendix A. SIMULATION PARAMETERS

In the simulation examples, all noises are defined as i.i.d. and unbiased. The true process noise is given by the parameter vector $\boldsymbol{\theta}^{\text{true}} = (\sigma_x^{-2}, \sigma_y^{-2}, \sigma_z^{-2}, \sigma_I^{-2}, \sigma_T^{-2}, \sigma_t^{-2})$ for the SD-IF model, and omits the last element in the DD-IF model, where $\sigma_x = \sigma_y = 0.01$ and $\sigma_z = \sigma_I = \sigma_T = \sigma_t = 0.001$. In the second simulation example, the erroneous model parameters are initialized such that $[\boldsymbol{\theta}^{\text{true}}]_i / [\boldsymbol{\theta}^{(0)}]_i \sim \mathcal{U}([10^{-1}, 10])$. The integer ambiguities are realized with $a = 10$ ambiguities and $b = 0.001$ cycle-slips/s, and the standard deviation of the code/phase/Doppler noises are defined with a standard deviation of 0.5/0.01/0.05, respectively. The standard deviation of the noise by which the measurement models ionosphere/troposphere/clock-biases are introduced is given by 0.01/0.01/0.001, respectively. A total number of 10 satellites are considered at all times with positions and velocities corresponding to the GPS constellation. All three frequency bands are used ($L_j \in \{L_1, L_2, L_5\}$) with $(f_1, f_2, f_5) = (1575.42, 1227.6, 1176)$ [MHz]. All experiments are run with periodic sampling at 0.2 [Hz], over $K = 10^3$ time steps. The relaxed estimate prior is

$$\mathcal{N}(\mathbf{z}_0; \mathbf{0}, \text{diag}(\mathbf{I}_3, 0.1))\mathcal{N}(\mathbf{n}_0; \mathbf{0}, \mathbf{I})\mathcal{N}(\boldsymbol{\xi}_0; \mathbf{0}, 0.01\mathbf{I})$$

where only the ambiguity distribution differs in the synthetic data, where we instead let $\mathbf{n}_0 \sim \mathcal{U}([-10, 10]^{\dim(\mathbf{n}_0)})$.